COMPONENT PART NOTICE

THIS PAPER IS A COMPONENT PART OF THE FOLLOWING COMPILATION REPORT:

TITLE: Engine Response to Distorted Inflow Conditions: Conference Proceedings of the Propulsion and Energetics Specialists' Meeting (68th) Held in Munich, Germany on 8-9 September 1986.

TO ORDER THE COMPLETE COMPILATION REPORT, USE AD-A182 635.

THE COMPONENT PART IS PROVIDED HERE TO ALLOW USERS ACCESS TO INDIVIDUALLY AUTHORED SECTIONS OF PROCEEDING, ANNALS, SYMPOSIA, ETC. HOWEVER, THE COMPONENT SHOULD BE CONSIDERED WITHIN THE CONTEXT OF THE OVERALL COMPILATION REPORT AND NOT AS A STAND-ALONE TECHNICAL REPORT.

THE FOLLOWING COMPONENT PART NUMBERS COMPRISE THE COMPILATION REPORT:

AD#: P005 462 thru P005 473 AD#: _____

AD#: _____ AD#: _____

AD#: _____ AD#: _____

Accession For	
NTIS GRA&I	☒
DTIC TAB	☐
Unannounced	☐
Justification	
By	
Distribution/	
Availability Codes	
Dist	Avail and/or Special
A-1	

DTIC FORM 463 MAR 85

OPI: DTIC-TID

TRANSMISSION OF INLET DISTORTION THROUGH A FAN

by

J E Flitcroft
J Dunham
W A Abbott

Royal Aircraft Establishment, Pyestock
Farnborough, Hants, GU14 0LS, UK

SUMMARY

The effect of inlet swirl on the propagation of total pressure distortion through a 3-stage fan without inlet guide vanes has been investigated on a compressor rig. The tests gave the unexpected finding that the presence of a swirl counter to the rotation of the fan generally reduced the level of steady state distortion transmitted to the core compressor. Dynamic pressure measurements made at the exit from the fan, however, revealed that the swirl also caused a sudden early breakdown of the flow in a sector of the hub region, resulting in high time-variant distortion levels in the core flow. This observation is compatible with the destabilising effect of a swirl counter to fan rotation on engines. A theoretical analysis confirmed that a swirl, concentrated at the fan tip at entry, could drive some of the hub blade rows strongly towards stall.

NOMENCLATURE

PT = Total pressure (kPa)

TT = Total temperature (^{o}K)

θ = Angular circumferential extent (degrees)

$$DC(\theta) = \frac{\text{Annulus or face mean total pressure} - \text{Lowest mean total pressure in a } \theta^{o} \text{ sector}}{\text{Dynamic head}}$$

$$PC(\theta) = \frac{\text{Annulus or face mean total pressure} - \text{Lowest mean total pressure in a } \theta^{o} \text{ sector}}{\text{Annulus or face mean total pressure}}$$

$$TC(\theta) = \frac{\text{Highest mean total temperature in a } \theta \text{ sector} - \text{Annulus mean total temperature}}{\text{Annulus mean total temperature}}$$

$$\text{Pressure distortion transfer ratio} = \frac{PC(\theta) \text{ fan exit}}{PC(\theta) \text{ fan inlet}}$$

$$\text{Temperature creation ratio} = \frac{TC(\theta) \text{ fan exit}}{PC(\theta) \text{ fan inlet}}$$

$$\text{Normalised PTIN} = \frac{\left[\frac{PT(\text{arm average})}{PT(\text{Annulus mean})} - 1\right] \text{ fan inlet}}{\left[1 - \frac{PT(\text{minimum arm average})}{PT(\text{annulus mean})}\right] \text{fan inlet}}$$

$$\text{Normalised PTDEL} = \frac{\left[\frac{PT(\text{arm average})}{PT(\text{annulus mean})} - 1\right] \text{ fan exit}}{\left[1 - \frac{PT(\text{minimum arm average})}{PT(\text{annulus mean})}\right] \text{fan inlet}}$$

$$\text{Normalised TTDEL} = \frac{\left[\frac{TT(\text{arm average})}{TT(\text{annulus mean})} - 1\right] \text{ fan exit}}{\left[1 - \frac{PT(\text{minimum arm average})}{PT(\text{annulus mean})}\right] \text{fan inlet}}$$

TU = Maximum RMS pressure fluctuation observed at an operating point (Radial average).

TU_{Max} = Maximum RMS pressure fluctuation observed (Radial average).

INTRODUCTION

During the development of the Tornado powerplant it became apparent that a swirl in the inlet flow, counter to the rotation of the engine ("contraswirl"), had a significant destabilising influence, substantially reducing the level of total pressure distortion that could be tolerated. The adverse effect of a circumferential variation in total pressure on engine stability is, of course, well established[1,2]. Although the solution adopted on the aircraft was to incorporate aerodynamic fences in the curved intake, in locations which inhibited the secondary flow behaviour responsible for the swirl[3], the situation had highlighted a lack of knowledge of the manner in which swirl affected engine stability. Since curved inlet ducts are frequently required for practical installations, a better understanding of the effect of swirl was clearly needed to enable its significance to be assessed fully for future powerplant designs.

A variety of explanations for the adverse effect of contraswirl were considered. One was the creation of a significant mismatch between the spools. However an examination of measurements on an engine showed that, although contraswirl caused a small reduction in the speed of the fan relative to the core, the operating point remained on a similar working line to that followed without swirl. Since the operating lines of the core compressors are established by choking of the HP turbine nozzle guide vanes, and are therefore insensitive to the fan exit conditions, there was no evidence for the mismatched spool hypothesis. Given that the surges had been observed to initiate in the core compressors rather than the fan it was clearly not just a consequence of the fact that contraswirl increased the incidence of the first blade row to the point where stall occurred; since the first blade row in this case was a rotor in practice only a small increase in incidence occurred. The only feasible explanation for the effect of contraswirl was therefore that it resulted in higher levels of flow distortion entering the core engine.

To test the above hypothesis, and provide data for the evaluation of prediction methods, measurements of the transmission of inlet total pressure distortion were made on a representative military fan. The results are presented in this paper. Although the stabilising influence of the core engine, due to the coupling between closely spaced spools, would not be represented in this experiment, it was anticipated that the correct trends would be obtained[4]. A theoretical analysis of the effect of swirl on the fan aerodynamics was also undertaken, to provide a qualitative means of assessing the changes likely to be taking place within the turbomachinery to produce the observed behaviour.

RIG DESCRIPTION

The general arrangement of the test rig is shown in Figure 1. Air is drawn in by the fan through an inlet silencer and calibrated air meter. A non-uniform inlet pressure distribution, representing an off-design aircraft intake flow pattern, was produced by inserting a gauze screen in the distortion generator. For tests without swirl the gauze was supported by a honeycomb mesh, Figure 2a. For investigations with swirl the honeycomb support was replaced by a series of radial vanes, which were twisted along their length to create a rotation which varied from 0° at the hub to a maximum at the tip, Figure 2b. The gauze blockage could be rotated through 350°.

The fan module comprised a 3 stage low-hub/tip ratio research machine without inlet guide vanes, representative of current military engine technology. The fan discharged into a split-flow collector box which incorporated two concentric dump diffusers. Both core and by-pass streams passed through airmeters prior to discharge through a common throttle valve. The fan by-pass ratio was pre-set using a bias gauze.

During the investigation it was discovered that the bend downstream of the dump diffusers produced a circumferential variation of the flow properties at the fan exit measurement plane. A subsequent comparison, using the measurements made with a single rake arm and rotating the blockage, showed that results obtained with a fixed gauze blockage could be corrected by considering the bias induced by the bend to be superimposed on the measured exit circumferential variation.

INSTRUMENTATION

Two types of inlet flow survey instrumentation were used; a symmetrical 8-arm array of rakes with 5 probes per arm, each probe incorporating a miniature pressure transducer and thus able to measure both time-averaged and time-variant total pressure, or a single arm containing five 5-hole conical yawmeter probes. The inlet rakes were removed when taking the definitive exit flow measurements with swirl. Fan delivery pressures were measured using 8 rakes, each containing 5 steady-state total pressure probes in both core and by-pass flow annuli. The centre probe in the by-pass and the second and fourth probe in the core on each arm contained a miniature pressure transducer for time-variant pressure measurement (Figure 3). The time-variant pressure signals were recorded on magnetic tape. The system was limited to 40 channels so when the delivery conditions were being recorded only 16 inlet probes could be monitored. Fan exit temperature was measured using a single rake with 4 thermocouples in each annulus.

TEST CONDITIONS

For the first phase of testing a range of throttle settings was examined at 80, 85 and 90% design speed with both clean and non-uniform inlet flow conditions. The swirl vanes and gauze were tested both separately and in combination. In the second phase of

the investigation the distortion generator was rotated in 30° increments to provide a full flow-survey at entry using the single yaw meter rake and at exit from the single temperature rake.

A structural loading limit on the inlet silencer system precluded surging of the fan during these tests.

DISCUSSION OF THE STEADY-STATE RESULTS

Fan inlet flow conditions

The gauze used to generate the circumferential pressure variation gave a once-per-revolution pattern. A contour plot is shown in Figure 4. There was no net swirl associated with the gauze alone. At the measurement plane the maximum deviations from axial flow, measured at the sides of the low pressure region, were less than $\pm 2^{\circ}$.

The swirl vanes in isolation gave a rotation counter to the fan which varied from 3° at 32% radius to 12° at 92% radius. In combination with the gauze, swirls of almost double the above levels were observed in the low pressure region, (Figure 5).

Fan overall operating characteristics

The overall performance of the fan with a clean inlet, and with the gauze and swirl vanes both separately and in combination, is summarised in Figure 6. The gauze and swirl combination produced a marked reduction in both flow and pressure ratio, a contrast to the limited change from the clean inlet performance observed with the gauze alone. The reduction in pressure ratio and flow with swirl alone as the fan was throttled was unexpected. Simple theory would indicate that a rotation in the flow in the opposite sense to the fan would normally result in the movement of the operating line to the right[4].

Distortion transmission without swirl

The steady-state distortion transmission behaviour of the fan measured with the gauze alone is illustrated in Figure 7. Normalised curves showing the circumferential variation of inlet total pressure, exit total pressure and exit temperature for core and by-pass regions are presented. For calculation purposes the inlet flow was divided into concentric circular stream tubes with the measured core/by-pass flow split. The greater attenuation of pressure distortion achieved in the by-pass region is clearly apparent, a finding consistent with the much steeper operating characteristic of that region of the fan (Figure 8). Both the core and by-pass flows exhibited peak temperatures in the region where, at inlet, the rotor was sweeping into a rising total pressure field, a feature seen by other workers[6,7]. A local increase in blade incidence occurs in the region, due to the tendency of the fan to induce a static pressure distortion ahead of the rotor, in sympathy with the total pressure variation[8].

The effect on the distortion transfer characteristics of fan speed and operating point are illustrated in Figure 9. Although the parameter used to characterise the transfer is based on a 60° sector angle, similar levels were obtained for a range of angles up to 135°. The results show little variation with fan speed. The initial increase in attenuation in the core as the fan is throttled, followed by a subsequent rise, was also observed in Reference 5. The consistently high levels of attenuation achieved in the by-pass region render it the more attractive location for engine control instrumentation for monitoring the fan working point, since such instrumentation needs to be relatively insensitive to the orientation of any inlet flow distortion.

The effect of swirl on distortion transfer

Figure 10 shows the equivalent inlet and exit flow measurements for the gauze and swirl combination at an equivalent operating condition to that illustrated for the gauze alone in Figure 7. Whilst the basic features are similar, it will be noted that the levels of attenuation achieved are greater. As Figure 11 shows this was also the case at the other operating conditions examined. On the above evidence it therefore appeared that a swirl counter to the rotation of the fan did not result in higher levels of circumferential distortion entering the core engine.

Since a strong radial variation in total pressure could also affect the surge margin of the core compressor, a comparison was made of the mean total pressures on each ring of probes. The magnitude of the local circumferential variation on each ring was also examined. Typical comparisons are shown in Figure 12. There was no indication that the tests with swirl produced a more severe hub-low pattern, which would be the most likely to cause a loss of core compressor stability. Furthermore, with swirl, the level of circumferential distortion was lower in the hub region than without swirl. The radial variation was also less. There was therefore no evidence that a swirl counter to the fan rotation caused a more adverse radial distortion.

From the tests where the blockage had been rotated to provide exit temperature surveys it was found that the levels of total temperature distortion in the fan core delivery region were also lower with contraswirl in combination with the gauze (Figure 13). Although when compared on the basis of pressure ratio the level with swirl does rise to equal the value measured with the gauze alone, it should be noted that the condition does relate to a higher operating point because of the adverse effect swirl had on overall fan performance.

Comparison with predictions

In the absence of a fully 3-D model the predictions of the steady-state distortion transfer were made using a linearised two-dimensional method, which models the upstream and downstream ducting and the fan as a series of control-volumes[4]. The mean flow properties in the fan control-volumes were calculated using a blade-row stacking model. The core and by-pass regions of the fan were treated as two separate machines, the location of the dividing streamline being determined using a streamline curvature calculation program. Only the mean value of circumferential swirl could be specified at the upstream boundary.

Examples of the measured and predicted exit profiles for the core region are presented in Figure 14 for cases both with and without swirl. Although there was generally good agreement in the basic shapes, the measured increase in attenuation observed with the swirl present in combination with the gauze was not correctly reproduced. A small decrease was usually indicated. In the by-pass region the predictions differed substantially from experiment because the calculated levels of attenuation were comparable with those for the core. The reason for this was apparently due to the predicted by-pass compressor characteristic having a lower slope than the measured one. A simple calculation using the slope of the measured characteristic gave levels of attenuation comparable with those observed in the experiment.

DISCUSSION OF THE DYNAMIC MEASUREMENTS

A comparison of the maximum values of Root Mean Square (RMS) pressure fluctuation measured in the core annulus at exit from the fan gave the first indication of a mechanism by which the presence of contraswirl could make conditions worse for the core turbomachinery. At all three speeds examined during the initial phase of testing a dramatic increase in turbulence was noted with the gauze and swirl combination as the fan was throctled to the highest operating point (Figure 15). In an engine this would result in a large rise in the level of time-variant distortion entering the core compressor, and would more than offset the slight reduction in steady-state distortion obtained with contraswirl. At lower operating points the much smaller increment in turbulence with contraswirl would only result in comparable peak instantaneous levels.

From the second phase of testing, where the blockage was rotated, it was evident that the peak turbulence occurred in the same region as the peak temperature and not the lowest steady-state pressure. A circumferential shift between the instantaneous peak and steady-state distortion patterns would therefore be indicated. As mentioned previously the location of the peak temperature corresponds to the region where at entry the local crossflow induced by the static pressure distortion, produced in sympathy with the total pressure variation by the rotor, leads to increased blade incidence. On the other side of the trough, where the induced swirl perturbation would be co-rotational, the levels of turbulence were similar to those obtained at lower operating points.

A comparison of the circumferential variation of steady-state total pressure in the core as the operating point was raised revealed that a marked local deterioration in fan performance had occurred in the region of high turbulence. As Figure 16 shows, at the highest operating point the left hand edge of the low pressure region was no longer clearly defined. A comparison of the respective inlet pressure and turbulence measurements showed no substantial difference, confirming that the observed behaviour was due to a local breakdown of flow within the fan. An examination of the associated transducer signals from the by-pass region confirmed that the effect was concentrated at the hub. Spectral analysis of the turbulence revealed a dominant sub-rotor speed frequency, in the manner of a rotating stall, which was not present at the other operating conditions.

Supporting evidence for the explanation that a local breakdown of flow in the hub region of the fan can occur without initiating surge directly, only to trigger it subsequently in the core turbomachinery, is provided by the findings of Miatt and Schaffler[9]. In that case, with a uniform inlet flow, surges of the HP compressor were induced by closing the nozzle to well below the normal operating area. The cause was found to be a rotating stall in the fan hub. The presence of a circumferential variation in inlet total pressure could be regarded as imposing a cyclic variation on such behaviour.

The absence of any inter-blade-row instrumentation on the fan meant that no evidence was available to indicate at what point within the fan the flow breakdown was occurring. Some guidance was however provided by a theoretical analysis of the effect of a circumferential swirl on the flow within the fan, using an axisymmetric streamline curvature computer program[10].

THEORETICAL ANALYSIS OF FAN INTERNAL AERODYNAMICS

The streamline curvature program required a specification of air outlet angle (or deviation) and pressure loss coefficient at the outlet from each blade row as a function of radius. Since this information was not available for the full range of conditions likely to arise in the presence of swirl, a representative specification, which matched the fan performance at a working line pressure ratio at 90% speed without swirl, was used for all calculations. Although the findings must therefore be regarded as providing a qualitative, rather than quantitative, guide to the effect of swirl on the internal flow behaviour, the correct trends were expected to be present.

Figure 17 shows the overall performance characteristics obtained. For comparison the measured characteristics are also presented. It is immediately obvious that with fixed loss coefficients the marked turnover of the measured characteristics is not obtained; since the measured pressure rise is lower, either the loss or deviation (or both) must be greater.

A possible justification for higher loss and/or deviation can be seen from the following table, showing the effect of inlet contraswirl on the local incidence angles at three radial stations, representative of hub, mean and tip conditions.

EFFECT OF SWIRL ON LOCAL INCIDENCE ANGLES

% N_D	BLADE ROW	HUB	MEAN	TIP
85	rotor 1	-0.4	+0.2	+0.2
	stator 1	+2.5	+0.7	-3.3
	rotor 2	+4.1	0	-0.5
	stator 2	+3.2	-0.9	-1.8
	rotor 3	+2.1	-0.3	-0.3
	stator 3	+0.8	-0.7	-0.6
90	rotor 1	-0.5	+0.2	+0.2
	stator 1	+2.9	+1.3	-2.9
	rotor 2	+4.9	+0.4	-0.5
	stator 2	+4.4	-0.2	-1.3
	rotor 3	+3.5	+0.2	0
	stator 3	+2.3	+0.2	+0.3

At each speed the pressure ratio was taken on the relevant working line. It is interesting to note that although the inlet swirl used in the calculation was zero at the hub, and increased linearly to a maximum of 10^{o} at the tip, it is the hub incidences which increase. This is because the axial velocity distribution has to adjust itself in order to maintain radial equilibrium.

The effect of these higher incidences is to increase significantly the loading parameter $\hat{}P/D$ (static pressure rise/inlet dynamic head) at the stator hub of stages 1 and 2 to values at which stall might well occur. The local axial velocity profile is also expected to deteriorate, as shown in Figure 18. It is relevant to note that if the calculations were repeated with the increased loss and deviation apparently indicated by the test results, the changes in incidence and axial velocity profile with swirl would have been greater.

The theoretical analysis in combination with the experimental results, provide a convincing explanation of how a contraswirl, concentrated at the fan tip at inlet, can result in a substantial deterioration of the quality of the flow entering the core compressors and in turn account for the increased sensitivity of the engine to inlet distortion.

CONCLUSIONS

Time-averaged measurements of the transmission of distortion through a split-flow military fan showed that, at fan exit in the by-pass region, the level of distortion was only about 20% of the value at inlet. Substantially less attenuation was achieved in core, with about 60% of the inlet value being measured. The effect of a swirl counter to the fan rotation was, surprisingly, favourable, increasing attenuation in the core so that the level of distortion at exit was now only about 45% of the inlet value.

Calculations of the steady-state distortion transmission behaviour, in the core predicted the circumferential variation well, but gave an incorrect indication of the effect of swirl.

The picture changed markedly when the dynamic content of the exit pressure distortion was taken into account. On the normal working line of the fan the addition of contraswirl resulted in turbulence more than three times the level observed with distortion alone. The large implied increase in the time-variant total pressure distortion in the flow entering the core compressors could well account for the observed reduction in stability margin of engines when subjected to distortion in combination with contraswirl. Calculations using an axisymmetric flow program showed that for this fan there was a strong tendency for inlet swirl to increase the incidences of blading in the hub, supporting the experimental evidence that the high turbulence was due to a local region of hub stall.

Dynamic instrumentation in the fan exit is clearly desirable in rig or engine tests where potential fan-core interactions are being examined.

ACKNOWLEDGEMENTS

The authors would like to acknowledge the assistance of Dr Hynes of the Whittle Laboratory, Cambridge who provided the theoretical calculations of distortion transfer for comparison with the experimental results, Mr McKenzie and Mrs Beaven of RAE Pyestock who helped with the testing and the analysis of the dynamic measurements respectively, and to colleagues at Rolls-Royce for helpful discussion of the aerodynamic analysis.

REFERENCES

1. Hercock R G, Williams D D — Aerodynamic response. AGARD LS72. Nov 1974

2. Bowditch D N, Coltrin R E — A survey of inlet/engine distortion compatibility. NASA TM 83421. June 1983

3. Stocks C P, Bissinger N C — The design and development of the Tornado engine air intake. AGARD CP301. May 1981

4. Ham C J, Williams D D — Some applications of Actuator and Semi-Actuator disk theory to the problems of intake/engine compatibility. IGTC-50. Tokyo 1983

5. Hercock R G — Effect of intake flow distortion on engine stability. AGARD CP234. October 1982

6. Mazzaway R S — Multiple segment parallel compressor model for circumferential flow distortion. ASME Journal of Engineering for Power. April 1977

7. Evans D G, de Bogdan C E, Soeder R H, Pleban E J — Some comparisons of the flow characteristics of a turbo-fan compressor system with and without inlet pressure distortion. NASA TMX-71574. July 1974

8. Plourde G A, Stenning A M — Attenuation of circumferential inlet distortion in multistage axial compressors. Journal of Aircraft Volume 5 No 3. May-June 1968

9. Schaffler A, Miatt D C — Experimental evaluation of heavy fan-high-pressure compressor interaction in a three shaft engine Parts 1 and 2. Papers 85-GT-173 and 85-GT-222 ASME 30th International Gas Turbine Conference, Texas - March 1985

10. D H Frost — A streamline curvature through-flow computer program for analysing the flow through axial-flow turbomachines. ARC R&M 3687 - 1972

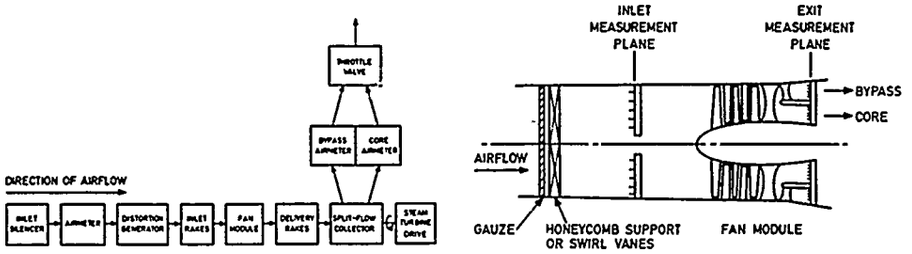

a. Block diagram of the rig arrangement

b. General arrangement of the main rig module

FIG 1 DETAILS OF THE RIG LAYOUT

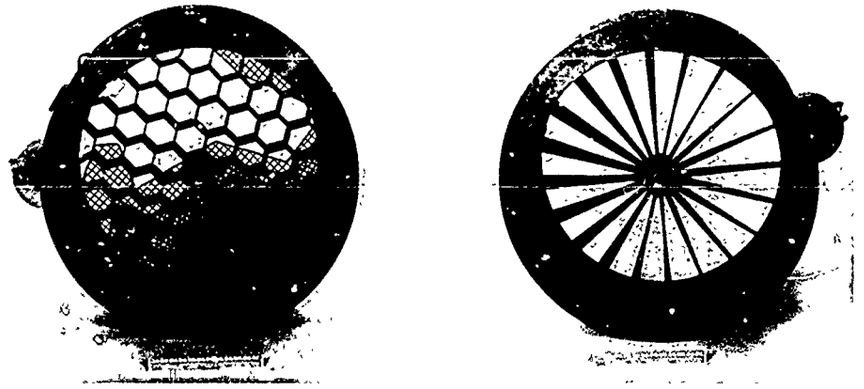

a. Gauze and honeycomb support

b. Swirl vanes

FIG 2 DISTORTION GENERATOR CONFIGURATIONS

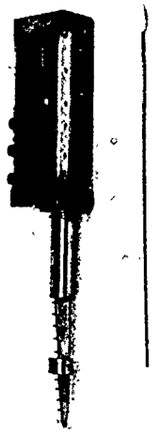

FIG 3 FAN DELIVERY TOTAL PRESSURE RAKE ARM

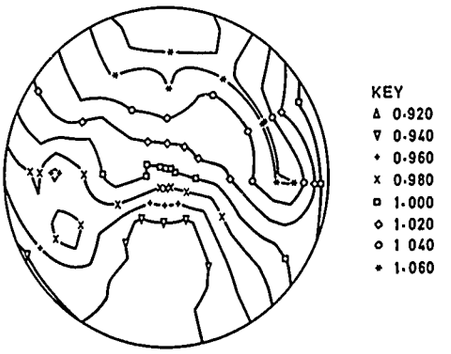

FIG 4 INLET TOTAL PRESSURE DISTRIBUTION WITH GAUZE

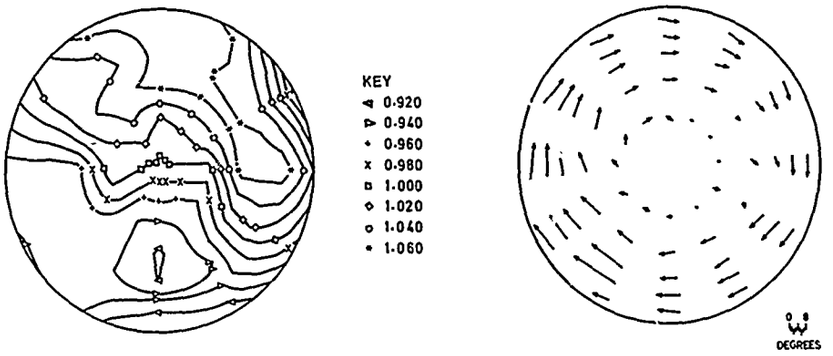

a. Normalised total pressure contours b. Swirl angle

FIG 5 INLET FLOW WITH GAUZE AND SWIRL

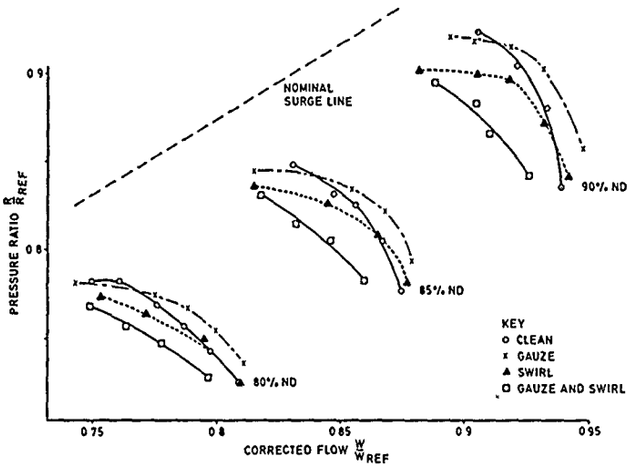

FIG 6 OVERALL FAN CHARACTERISTICS

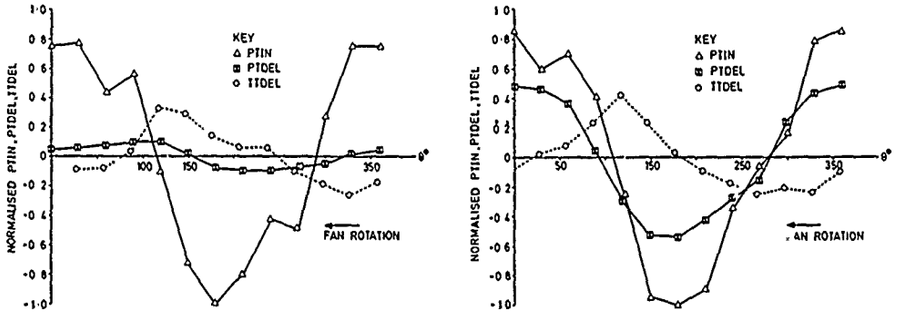

a. Bypass b. Core

FIG 7 GAUZE ALONE, 90% SPEED

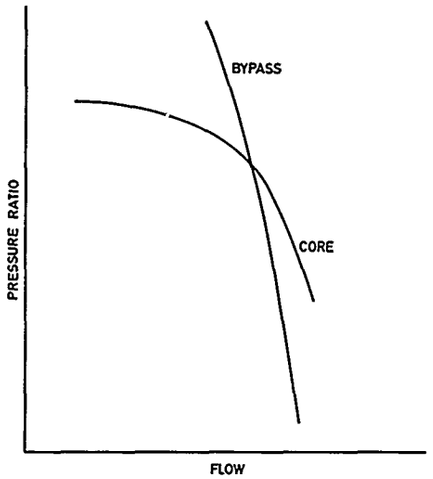

FIG 8 EXAMPLE SPLIT-FLOW CHARACTERISTIC

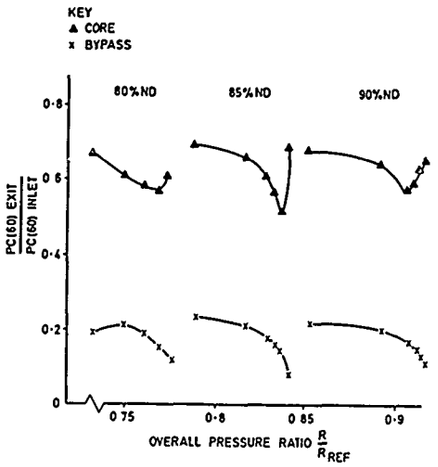

FIG 9 PRESSURE DISTORTION TRANSFER BEHAVIOUR WITH GAUZE

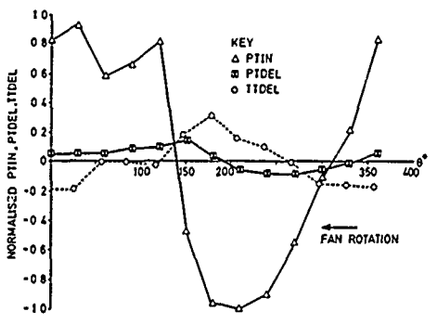

a. Bypass

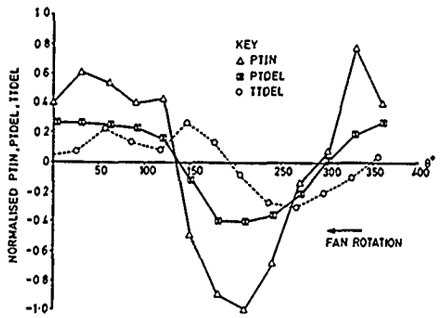

b. Core

FIG 10 GAUZE AND SWIRL, 90% SPEED

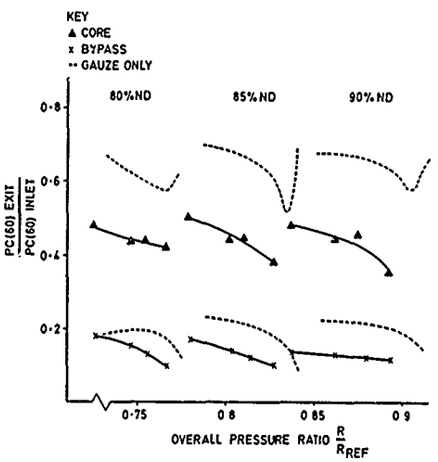

FIG 11 PRESSURE DISTORTION TRANSFER BEHAVIOUR WITH GAUZE AND SWIRL

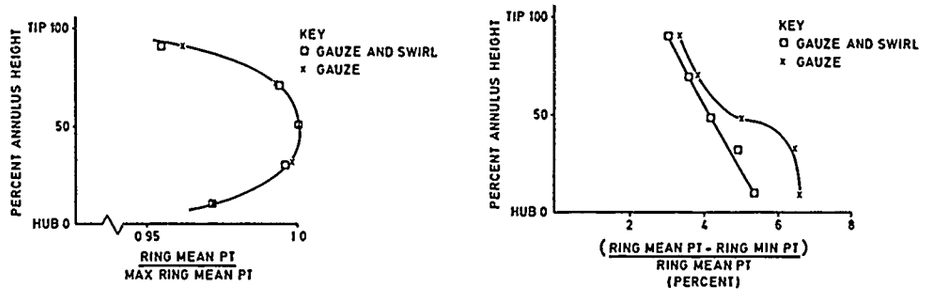

a. Ring mean total pressure

b. Circumterential variation on a ring

FIG 12 COMPARISON OF RADIAL PROFILES IN THE CORE ANNULUS

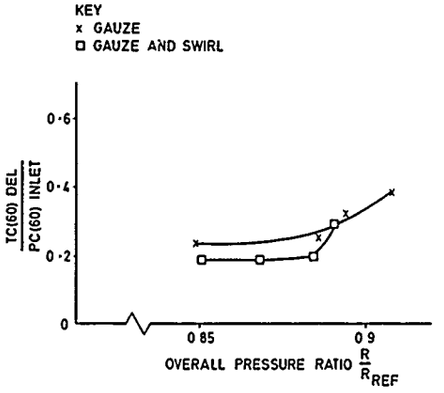

FIG 13 CORE TEMPERATURE DISTORTION COMPARISON FOR 90% SPEED

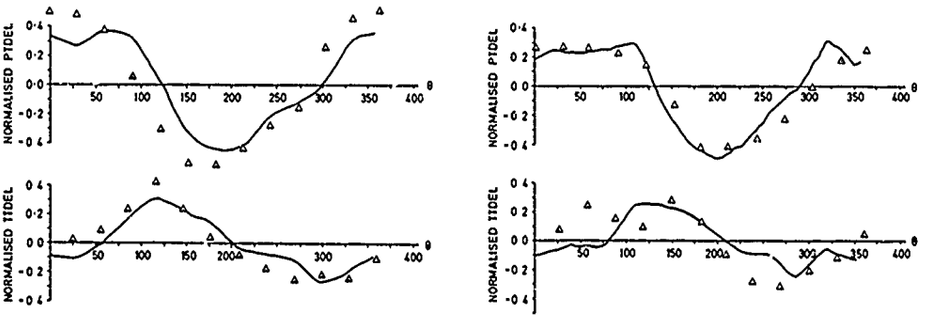

a. Gauze

b. Gauze and swirl

FIG 14 COMPARISON WITH PREDICTIONS

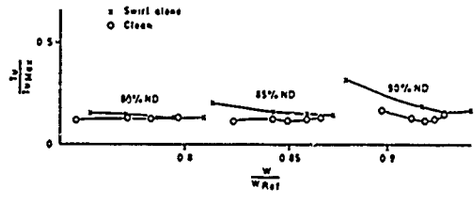

(a) Comparison for clean and swirl alone

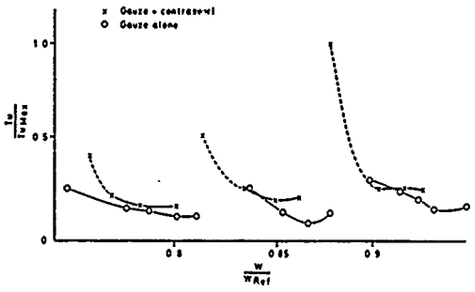

(b) Comparison for gauze and gauze + contraswirl

FIGURE 15 THE VARIATION OF CORE EXIT TURBULENCE WITH SPEED AND OPERATING POINT

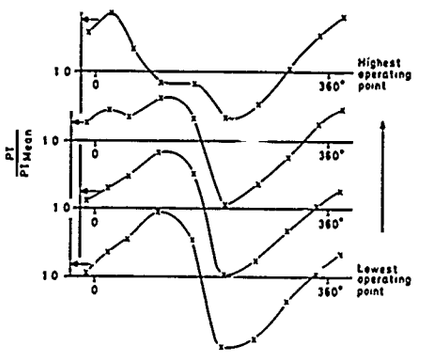

FIGURE 16 VARIATION OF CORE EXIT PRESSURE WITH OPERATING POINT (GAUZE + CONTRASWIRL)

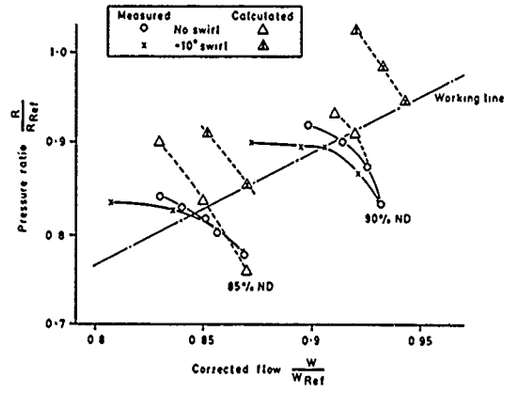

FIGURE 17 PREDICTED COMPRESSOR CHARACTERISTICS

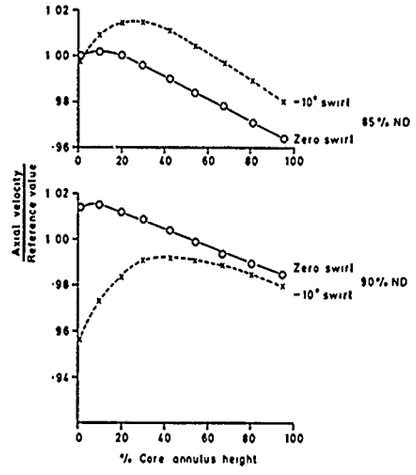

FIGURE 18 OUTLET AXIAL VELOCITY PROFILE (CALCULATED)